Anomalous low-frequency butterfly curves for subsidiary and ferromagnetic resonance overlap at 3 GHz

R. W. Cross
National Institute of Standards and Technology, Boulder, Colorado 80303

C. E. Patton, G. Srinivasan, J. G. Booth, and M. Chen
Department of Physics, Colorado State University, Fort Collins, Colorado 80523

(Received 31 August 1990; accepted for publication 18 October 1990)

Subsidiary absorption butterfly curves of spin-wave instability threshold versus static in-plane field have been obtained for yttrium iron garnet (YIG) thin films at 3 GHz. The butterfly curves have been found to be rather anomalous, typically displaying a pronounced dip and a very low minimum threshold. These anomalous features are attributed to the overlap of the subsidiary absorption field region with ferromagnetic resonance (FMR). First-order instability theory was extended to include the uniform mode response near FMR. The extended theory yields good fits to the data for reasonable values of the YIG FMR linewidths. The theoretical analysis also shows a predicted flip in the azimuthal propagation angle ϕ_k for the unstable spin waves in the region of FMR overlap. With increasing field, there are predicted discontinuous changes in ϕ_k from 90° to 0° and back to 90° in the region of FMR.

I. INTRODUCTION

A combination of microwave and Brillouin light scattering (BLS) techniques has been used recently to study spin-wave instability processes in yttrium iron garnet (YIG) films.[1,2] The microwave measurements yield so-called butterfly curves of the spin-wave instability threshold h_{crit} versus static field H. The BLS technique allows for the identification of the specific spin-wave modes that become unstable. The initial work was done at 8–10 GHz. The correlation with theory was good, with two notable exceptions. First, the data showed no evidence for a predicted flip in the azimuthal spin-wave propagation angle ϕ_k for the unstable spin waves. Second, the measured magnon wave numbers at high fields were inconsistent with the theoretical values. The experiments were extended to low microwave frequencies with the intention of making direct observations of the predicted flips in the azimuthal spin-wave angle ϕ_k for the unstable modes. However, the main effect of using lower frequencies was to produce anomalous butterfly curves with very low minimum thresholds and pronounced dips.

The focus of this work is on the measurement and understanding of these "anomalies." The anomalies have now been attributed to the overlap of ferromagnetic resonance (FMR) at the pump frequency ω_p and subsidiary absorption for the unstable $\omega_p/2$ spin waves. Damping of the uniform mode at FMR has been included in the analysis and the first-order instability theory has been extended to include FMR overlap. The extended theory agrees with the data for reasonable YIG linewidth values. The analysis also reveals a new prediction of a flip in the azimuthal angle ϕ_k in the region of FMR overlap.

II. EXPERIMENT

The sample used for the measurements reported here was a 9.8-μm-thick yttrium-iron-garnet (YIG) film on a gadolinium-gallium-garnet substrate. The static field H and linearly polarized microwave field h_0 were both applied in the film plane, but orthogonal to each other as shown in Fig. 1. Figure 1 also shows the pertinent spin-wave wave vector $\mathbf{k}$. The angles θ_k and ϕ_k are the polar and azimuthal propagation angles for wave vector $\mathbf{k}$, respectively. A butterfly curve for subsidiary absorption with no FMR overlap is shown in Fig. 2 for a pump frequency of 8.5 GHz. The solid circles represent the experimental results and the curve represents a theoretical fit to the data, based on the first-order theory with no special treatment of FMR.[3] The fit is good and represents the typical high-frequency situation. In this range, first-order instability theory[3,4] is consistent with experimental observations with the two exceptions noted in the Introduction.

The work reported here focuses on the same basic experiment, but at lower microwave frequencies. A stripline transducer was used to generate the microwave pump field at 3 GHz. Figure 3 shows a typical butterfly curve for the YIG film. Note that the vertical axis in Fig. 3 shows only relative threshold value $\tilde{h}_{crit}$. It was not practical to obtain an accurate calibration of the absolute microwave field amplitude versus stripline power. The experimental data show a pronounced dip in the minimum threshold region. This dip is very different from the relatively flat minimum threshold region in Fig. 2. A theoretical curve calculated from the first-order theory of Refs. 3 and 4 is also shown. The scaling for the theory is the same as for the curves in Figs. 4 and 5, and will be discussed shortly. The main point of comparison here is that the theoretical curve has a very sharp dip which goes to zero at the butterfly curve minimum. The pronounced dip in the threshold field data and the zero-threshold value from the theory are attributed to FMR overlap. The narrow linewidth for YIG, with a corresponding sharp FMR profile, produces the experimentally observed dip. The zero-threshold limit in the theory is

 0021-8979/91/031569-05$03.00 © 1991 American Institute of Physics

Downloaded 26 Dec 2001 to 129.82.140.114. Redistribution subject to AIP license or copyright, see http://ojps.aip.org/japo/japcr.jsp

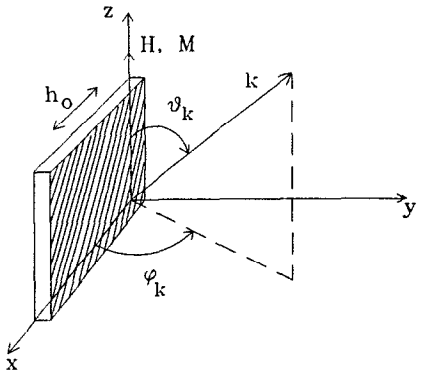

FIG. 1. Coordinate system and geometry for the thin film of magnetization M, with static field H, microwave field h_0, spin-wave vector k, and spin-wave propagation angles θ_k and ϕ_k.

due to neglect of damping. For zero damping, the uniform mode response diverges at FMR, thereby pushing the instability threshold to zero.

As indicated above, the source of these anomalies is FMR overlap. For FMR in YIG with the static field in-plane, resonance occurs at approximately 40 kA/m (500 Oe) for a pump frequency of 3 GHz, precisely at the position of the dip in Fig. 3. At 8.5 GHz, FMR occurs well above the field range for subsidiary absorption, there are no FMR effects, and the butterfly curve minimum is smooth and flat, as in Fig. 2. A proper treatment of the uniform mode response, which includes damping, is needed in order to fit the theory to experimental data for cases in which FMR overlap occurs. Such a treatment and the corresponding extension of the first-order theory which includes FMR overlap is summarized below.

III. THEORY

The basic first-order spin-wave instability theory was first developed by Suhl[5] and Schlömann.[6] In subsidiary

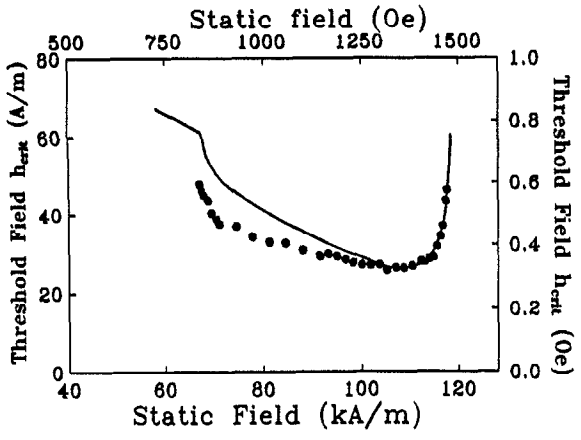

FIG. 2. Subsidiary absorption butterfly curve of threshold field amplitude h_{crit} vs in-plane static field for the 9.8-μm YIG film at 8.5 GHz. The solid circles indicate measured values. The curve is from the theory in Refs. 3 and 4.

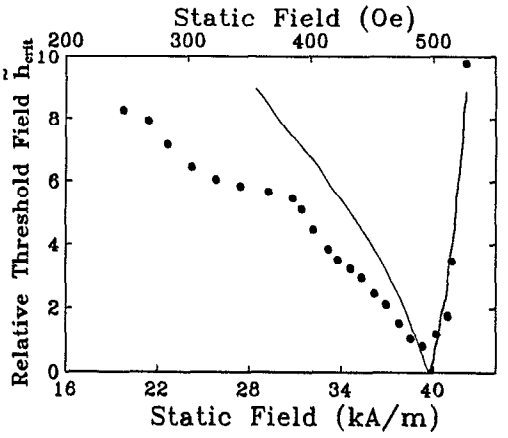

FIG. 3. Subsidiary absorption butterfly curve of relative threshold field amplitude $\bar{h}_{crit}$ vs in-plane static field for the 9.8-μm YIG film at 3 GHz. The solid circles indicate measured values. The curve is from the theory in Refs. 3 and 4.

absorption, the uniform mode at a pump frequency ω_p couples to the spin-wave modes at $\omega_k = \omega_p/2$. At a critical power and corresponding microwave field amplitude h_c, the power into the spin wave modes at (k, θ_k, ϕ_k) equals the rate of decay out of the modes. The observed instability threshold h_{crit} corresponds to the minimum possible h_c value among all available modes at $\omega_k = \omega_p/2$. Experimentally, one observes an abrupt increase in loss when the microwave field exceeds h_{crit}; h_{crit} is termed the instability threshold.

The uniform mode plays a key role in subsidiary absorption. The usual situation at 8.5 GHz is such that FMR

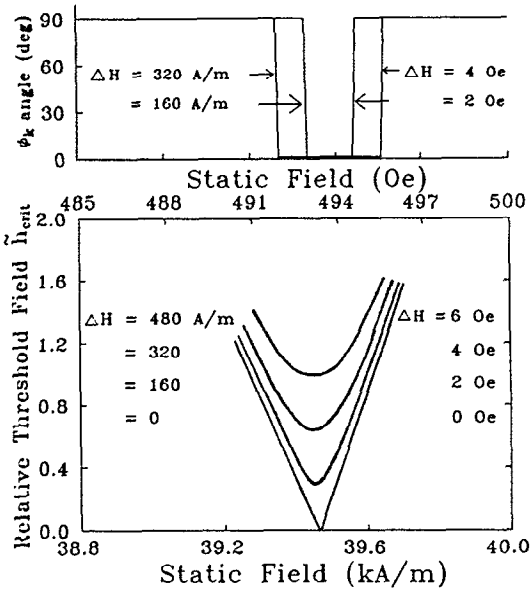

FIG. 4. Subsidiary absorption 3-GHz butterfly curves of threshold field $\bar{h}_{crit}$ vs static field in the region of the dip. The curves are from the theory for various values of FMR linewidth ΔH. The upper portion of the figure shows the theoretical predictions for the azimuthal propagation angle for the unstable spin waves.

Downloaded 26 Dec 2001 to 129.82.140.114. Redistribution subject to AIP license or copyright, see http://ojps.aip.org/japo/japcr.jsp

occurs at fields well above the subsidiary absorption field region. In such cases, it is necessary to consider the uniform mode response only for the low-field tail of the FMR absorption. In this region, the mode response is largely insensitive to damping or linewidth considerations, and such damping may safely be neglected in the theoretical analysis. This is usually the case for subsidiary absorption in ferrites at moderately high microwave frequencies. The theory in Ref. 3 was for this situation. However, as pointed out in Refs. 5 and 6, for certain sample shapes and pump frequencies, it is possible for the FMR peak to move into the field region for subsidiary absorption. Technically, this means that the subsidiary absorption is no longer "subsidiary" but rather overlaps with FMR. In any case, a proper theoretical treatment requires the inclusion of damping in the uniform response. This calculation was made in Refs. 5 and 6, but only for specific sample geometries and only at FMR.

The complex uniform precession response α_0 may be expressed in terms of the Larmor and anti-Larmor contributions,[3]

$$\alpha_0=(\gamma h_0/2)[q_L\exp(i\omega_p t)+q_A\exp(-i\omega_p t)], \quad (1)$$

where γ is the gyromagnetic ratio, h_0 is the amplitude of the microwave field, and $q_{L,A}$ denote the complex Larmor and anti-Larmor precession responses, respectively. The specific $q_{L,A}$ expressions in Ref. 3 include no damping terms and are valid at fields far from FMR. Damping may be taken into account in a straightforward manner by allowing the FMR frequency to be complex.[7] The conventional FMR frequency can be expressed as

$$\omega_{\rm res}=(XY)^{1/2}, \quad (2)$$

where X and Y are stiffness frequencies given by

$$X=\gamma(H+B_sN_x) \quad (3)$$

and

$$Y=\gamma(H+B_sN_y). \quad (4)$$

Here, H is the static internal field, B_s is the saturation induction, and $N_{x,y}$ are transverse demagnetization factors for a general ellipsoidal sample. The range of $N_{x,y}$ is given by $0<N_{x,y}<1$ in SI units The complex FMR frequency is expressed as

$$\Omega_{\rm res}=\omega_{\rm res}+i\eta_0, \quad (5)$$

where η_0 is taken as the uniform mode relaxation rate. The two corresponding stiffness frequencies must also be taken to be complex, according to

$$X\rightarrow X+i\Gamma_0 \quad (6a)$$

and

$$Y\rightarrow Y+i\Gamma_0, \quad (6b)$$

where Γ_0 is obtained from self-consistency:

$$\Gamma_0=2\eta_0(XY)^{1/2}/(X+Y). \quad (7)$$

These substitutions lead to modified expressions for $q_{L,A}$ which include the effect of damping. The substitutions need only be carried through for terms that have significant effects on the response. When this is done, the modified q_L and q_A functions become

$$q_L=\frac{(Y+\omega_p)a_x\exp(i\delta_x)+i(X+\omega_p)a_y\exp(i\delta y)}{(XY-\omega_p^2)+i\eta_0[(XY)^{1/2}+\omega_p]} \quad (8a)$$

and

$$q_A=\frac{(Y-\omega_p+i\Gamma_0)a_x\exp(-i\delta_x)+i(X-\omega_p+i\Gamma_0)a_y\exp(-i\delta y)}{(XY-\omega_p^2)+i\eta_0[(XY)^{1/2}+\omega_p]}. \quad (8b)$$

In the above expressions, ω_p is the pump frequency, and $a_{x,y,z}$ and $\delta_{x,y}$ are microwave field amplitude component and phase parameters from Ref. 3. These equations reduce to the standard $q_{L,A}$ expressions in Ref. 3 when η_0 and Γ_0 are set to zero. The effect of damping is the obvious one, to keep the resonance denominator in the $q_{L,A}$ terms from going to zero at resonance. If damping is not included, the uniform precession response diverges at FMR and pushes the instability threshold to zero.

The remaining steps in the analysis are the same as in Ref. 3. The threshold field amplitude for a given mode at $\omega_k=\omega_p/2$ and wave vector $\mathbf{k}$ is given by

$$h_c=(\omega_p/\omega_m)(\Delta H_k/|W|), \quad (9)$$

where ω_m is equal to γB_s and ΔH_k is the spin-wave linewidth. The coupling parameter W is given by

$$W=\sin\theta_k\cos\theta_k\{q_L[f(\theta_k)+\omega_p/2]\exp(-i\phi_k)+q_A^*[f(\theta_k)-\omega_p/2]\exp(i\phi_k)\}+\sin^2\theta_k a_z, \quad (10)$$

where the function $f(\theta_k)$ is

$$f(\theta_k)=[(\omega_m^2\sin^4\theta_k+\omega_p^2)^{1/2}-\omega_m\sin^2\theta_k]/2. \quad (11)$$

In Eqs. (10) and (11), θ_k and ϕ_k are the polar and azimuthal propagation angles for the spin wave. Note that the above expressions are based on the condition $\omega_k=\omega_p/2$. The available $(k,\ \theta_k,\ \phi_k)$ modes are constrained by the spin-wave dispersion,

$$\omega_k=\omega_p/2=[(H+Dk^2)(H+Dk^2+M\sin^2\theta_k)]^{1/2}, \quad (12)$$

where $k=|\mathbf{k}|$. The function $f(\theta_k)$ in Eq. (11) is actually the solution of Eq. (12) for $\gamma(H+Dk^2)$ as a function of θ_k, where D is the usual exchange stiffness field.

The experimentally observed $h_{\rm crit}$ threshold should correspond to the minimum value of h_c with respect to θ_k

Downloaded 26 Dec 2001 to 129.82.140.114. Redistribution subject to AIP license or copyright, see http://ojps.aip.org/japo/japcr.jsp

and ϕ_k. It is important to realize that the spin-wave linewidth ΔH_k is also a function of k and θ_k. The expression used here for the spin-wave linewidth is

$$\Delta H_k = A_0 + A_1 \sin^2 \theta_k + B_1 L(k/B_2), \quad (13a)$$

where $L(k/B_2)$ is given by

$$L(x) = 0.72 \ln[1 + 8x^2(1 + 2x^2)/(1 + 8x^2)], \quad (13b)$$

and A_0, A_1, B_1, and B_2 are used as fitting parameters. Equation (13a) has a theoretical basis, but is also somewhat empirical.[4] Subject to the constraints on the available spin-wave states at $\omega_k = \omega_p/2$ for any particular static field, sample field, shape, and orientation, the observed threshold h_{crit} will be the h_c for the particular (k, θ_k, ϕ_k) combination which minimizes $\Delta H_k/|W|$. It is important to note that the calculation of the minimum threshold field leads to very specific θ_k, ϕ_k, and k values for the parametric spin waves which are driven unstable just above h_{crit}.

For the pumping configuration shown in Fig. 1, δ_x, a_y, N_x and a_z are zero and a_x and N_y are equal to unity. For subsidiary absorption and main resonance overlap to occur, the FMR field for resonance at ω_p must be below the field at which the bottom of the spin-wave band coincides with $\omega_p/2$. For the thin films with in-plane fields, this condition reduces to

$$\omega_p < (2/3)\omega_m. \quad (14)$$

For YIG films, subsidiary absorption and FMR overlap occurs for a pump frequency below 3.28 GHz. Specific results based on the extended first-order theory are presented in the next section.

IV. ANALYSIS AND DISCUSSION

Figure 4 shows the effect of uniform mode damping on the theoretical butterfly curve in the region of the dip evident in Fig. 3. Curves of the relative theoretical $\tilde{h}_{\text{crit}}$ as a function of static field H are shown for a pump frequency of 3 GHz and selected values of the YIG FMR half-power linewidth ΔH. Linewidth and relaxation are connected by the relation $\Delta H = 2\eta_0/\gamma$. As is evident from Fig. 4, the dip becomes wider and the minimum h_{crit} value increases as ΔH is increased. This behavior is the quantitative effect of the decrease in the uniform mode response with increasing damping. As seen from these results, the shape of the experimental dip can be modeled reasonably well by including damping in the theory.

Figure 5 shows an overall comparison of the theoretical butterfly curve for $\omega_p = 3$ GHz and $\Delta H = 160$ A/m (2 Oe) with the data in Fig. 3. The theoretical fit was obtained by choosing the FMR linewidth ΔH which best modeled the shape of the experimental minimum, selecting the A_0 parameter in Eq. (13a) for ΔH_k to fit the minimum relative threshold to the data, and then adjusting the parameters A_1, B_0, and B_2 to fit the low- and high-field portions of the data. Apart from the linewidth (ΔH) effect, this is basically the procedure used in Ref. 4. Because the data are only for relative threshold values, the linewidth parameters A_0, A_1, B_0, and B_1 are also relative and contain

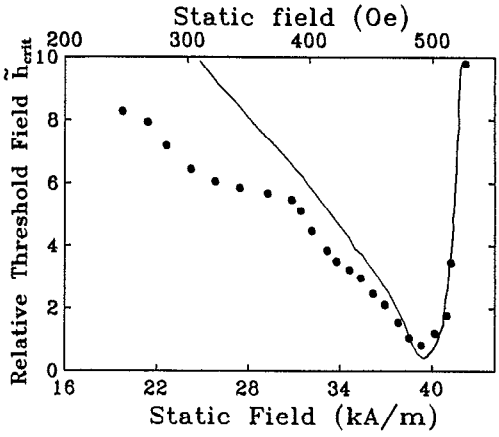

FIG. 5. Subsidiary absorption 3-GHz butterfly curve of the relative threshold $\tilde{h}_{\text{crit}}$ vs static field. The curve is from the theory for a FMR linewidth of 160 A/m (2 Oe). The solid circles repeat the experimental results from Fig. 3.

an undetermined scale factor. The fit is good above $H = 32$ kA/m (400 Oe). These results show that (1) the "anomalous" dip in the data is due to FMR overlap, and (2) the zero minimum threshold in the theory is removed when damping is included in the analysis.

As noted in the previous section, the theoretical value of h_{crit} is obtained by a minimization procedure over the available spin waves at $\omega_k = \omega_p/2$. This procedure leads to specific values for θ_k, ϕ_k, and k for the minimum threshold unstable mode. The analysis that yields the theoretical curves in Figs. 4 and 5 also yields an interesting result with regard to ϕ_k^{crit}, the azimuthal angle of the minimum threshold mode. This result is indicated schematically in the upper portion of Fig. 4, which shows the theoretical dependence of ϕ_k^{crit} on static field in the dip region. At fields below the dip region, the minimum threshold occurs for $\phi_k^{\text{crit}} = 90°$. In the dip region and over a range of static field on the order of ΔH, ϕ_k^{crit} flips to 0°. As H is increased further, ϕ_k^{crit} flips back to 90°. With reference to the YIG film spin-wave geometry in Fig. 1, it is clear that this ϕ_k flip is significant. The spin-wave propagation wave vector k is out-of-plane outside the dip region and flips in-plane around FMR overlap. It should be possible to observe this ϕ_k flip directly by BLS techniques.

ACKNOWLEDGMENTS

The authors gratefully acknowledge Dr. J. D. Adam, Westinghouse Research and Development Center, Pittsburgh, PA, for the YIG films used in this work. The stripline transducer was provided by Dr. W. Ishak, Hewlett Packard Laboratories, Palo Alto, CA. This work was supported in part by the Electromagnetics Directorate of the Rome Air Development Center, U. S. Air Force, under contract No. F19628-85-0002. J. G. Booth is with the Department of Pure and Applied Physics, University of Salford, Salford M5 4WT, UK. This work was performed, in part, while he was a visiting professor at Colorado State University.

Downloaded 26 Dec 2001 to 129.82.140.114. Redistribution subject to AIP license or copyright, see http://ojps.aip.org/japo/japcr.jsp

[1] W. D. Wilber, Ph. D. thesis, Colorado State University, 1987.
[2] W. D. Wilber, J. G. Booth, C. E. Patton, G. Srinivasan, and R. W. Cross, J Appl. Phys. **64**, 5477 (1988).
[3] C. E. Patton, J. Appl. Phys. **40**, 2837 (1969).
[4] C. E. Patton and W. Jantz, J. Appl. Phys. **50**, 7082 (1979).
[5] H. Suhl, J. Phys. Chem. Solids **1**, 209 (1957).
[6] E. Schlömann, J. J. Green, and U. Milano, J. Appl. Phys. **31**, 386S (1960).
[7] C. E. Patton, in *Magnetic Oxides*, edited by D. J. Craik (Wiley, London, 1975), pp. 575–645.

Downloaded 26 Dec 2001 to 129.82.140.114. Redistribution subject to AIP license or copyright, see http://ojps.aip.org/japo/japcr.jsp